Korean J. Chem. Eng., 32(2), 335-341 (2015)
DOI: 10.1007/s11814-014-0219-8

pISSN: 0256-1115
eISSN: 1975-7220

Adsorption equilibrium and kinetic studies of crystal violet and naphthol green on torreya-grandis-skin-based activated carbon

Wei Dai*,†, Huijing Yu*, Na Ma, and Xiaoyang Yan***

*College of Chemistry and Life Science, Zhejiang Normal University, Zhejiang Province Jinhua 321004, P. R. China
**College of Geography and Environmental Sciences, Zhejiang Normal University,
Zhejiang Province Jinhua 321004, P. R. China
(*Received 27 April 2014 • accepted 30 July 2014*)

Abstract−A new type of activated carbon, torreya-grandis-skin-based activated carbon (TAC), has been used to remove the harmful dyes (cationic dye crystal violet (CV) and anionic dye naphthol green (NG)) from contaminated water via batch adsorption. The effects of solution pH, adsorption time and temperature were studied. The Langmuir and Freundlich adsorption models were used to describe the equilibrium isotherm and isotherm constant calculation. It was found that the maximum equilibrium adsorption capacities were 292 mg/g and 545 mg/g for CV and NG, respectively. Adsorption kinetics was verified by pseudo-first-order, pseudo-second-order and intra-particle diffusion kinetic models. Results indicated that the rate of dye adsorption followed pseudo-second-order kinetic model for the initial dye concentration range studied. Temperature-dependent adsorption behavior of CV and NG shows that the adsorption is spontaneous and endothermic, accompanying an entropy increase. This work indicates that TAC could be employed as a low-cost alternative for the removal of the textile dyes from effluents.

Keywords: Adsorption, Crystal Violet, Naphthol Green, Torreya Grandis Skin, Activated Carbon

INTRODUCTION

Wastewater effluents containing synthetic dyes may cause potential toxic and carcinogenic effects to human health and environment [1]. Therefore, different methods such as precipitation, ion-exchange, adsorption, coagulation/ flocculation, advanced oxidation, ozonation, membrane separation and liquid-liquid extraction have been used to remove dyes from wastewater [1]. Conventional biological treatment methods are ineffective for decolorization because they are very stable against light and oxidation reactions [2]. Other commonly used techniques for dye decolorization include flocculation, membrane filtration, and reverse osmosis. However, these methods are merely transferring the contaminants from liquid phase to other media and causing secondary pollution [3]. Photocatalytic oxidation is a destructive technology leading to the total mineralization of most organic dyes. The drawbacks of photocatalytic oxidation technology are mainly the ineffective utilization of economic and ecological sunlight and high electron-hole pair recombination rate [4].

Adsorption is a very effective separation technique that now is considered to be superior to other techniques for water treatment in terms of initial cost, simplicity of design, ease of operation and insensitive to toxic substances. Activated carbon has proven to be an effective adsorbent for the removal of a variety of organic and inorganic pollutants dissolved in aqueous media or from gaseous environment [5]. Additionally, the other applications of activated carbon in the market are also vast, for example, serving as catalysts and catalyst supports. Agricultural wastes are considered to be a very important feedstock because they are renewable sources and low-cost materials [6]. Therefore, in recent years, many studies have examined the preparation of activated carbon from low-cost and readily available materials, mainly industrial and agricultural byproducts. Such alternatives include maize cobs waste [7], montmorillonite [8], fly ash [9], mansonia wood sawdust [10] and sunflower seed hull [11].

Torreya grandis, a subtropical plant, grows widely in Zhejiang Province of China [12]. Torreya grandis wine is a favorite health drink [13], but many skin residues are produced during the production process. As waste materials, the skin residues of torreya grandis have to be disposed as garbage, which can also sometimes cause another environment problem. In our previous work [14], torreya-grandis-skin-based activated carbon (TAC) was successfully prepared from torreya grandis skin residues.

On the other side, crystal violet (CV) is a water-soluble cationic dye, commonly present in effluent discharges form textile, food, pharmaceutical, printing and paper manufacturing industries [15]. In addition, naphthol green (NG) is one of the most common anionic dying materials for wood, silk and cotton [16]. The structures of CV and NG are shown in Scheme 1. Though CV and NG are not highly hazardous, they can cause some harmful effects. Acute exposure to CV and NG can cause increased heart rate, vomiting, shock, cyanosis, quadriplegia, and tissue necrosis in humans [17]. Thus, removal of CV and NG from wastewater and/or process effluent is very important due to their potential toxicity to human and environment. CV and NG for the reasons stated above were selected in this study as the model dyes.

†To whom correspondence should be addressed.
E-mail: daiwei@zjnu.edu.cn

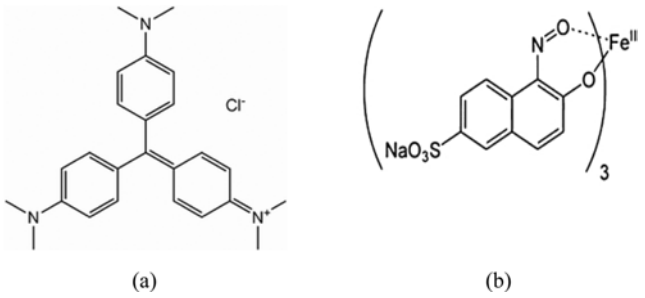

Scheme 1. Chemical structures of CV (a) and NG (b).

We report here the adsorption of a cationic dye crystal violet (CV) and anionic dye naphthol green (NG) over a new type of activated carbons (TAC). Removal of both cationic and anionic dyes is not readily achieved simultaneously and the adsorption can be understood much by a comparison between the two adsorbates. Adsorptive equilibrium isotherms, kinetics, and thermodynamics were processed to understand the adsorption mechanism of the dyes molecules onto the TAC. The aim behind using waste materials as an alternative low-cost precursor to prepare activated carbon is that it will provide a twofold advantage with respect to environmental pollution. On one hand, the huge volume of waste materials (skin residues of torreya grandis) and the cost of the waste disposal could be partly reduced and helped reduce the cost of waste disposal. On the other hand, the low-cost adsorbent, if developed, can provide a potentially inexpensive raw material for commercial activated carbon and reduce the pollution of wastewaters at a reasonable cost.

EXPERIMENTAL

1. Adsorbate and Solution

Crystal violet (CV) and naphthol green (NG), purchased from Sigma-Aldrich Company, were used without any further purification. The initial pH was adjusted with NaOH or HCl solutions. All of the reagents were analytical reagent grade. An aqueous stock solution of CV and NG was prepared by dissolving accurately weighed amounts of CV and NG in deionized water. The desirable experimental concentrations of solutions were prepared by diluting the stock solution with deionized water when necessary. We used three sets of parallel samples in the experiments. The average value of three sets of experimental data is used in the final graphic presentation. It was found that the resultant data was very reproducible in this work and the experimental deviation is within 3-5%.

2. Preparation and Nitrogen Adsorption of TAC

TAC was prepared by a patented KOH activation procedure [14] that was previously proposed by our group. Nitrogen adsorption-desorption isotherms were measured using a Micromeritics ASAP2020 analyzer. The specific surface areas were calculated using the BET equation by assuming a section area of nitrogen molecule to be 0.162 nm^2. The t-plot method was applied to calculate the micropore volumes and surface areas. The total pore volume was estimated to be the liquid N_2 volume at a relative pressure of 0.99. The pore size distribution was calculated by density functional theory (DFT). The nitrogen adsorption isotherm and the pore size distribution curve of TAC at 77 K are shown in Fig. 1. The sample shows a type

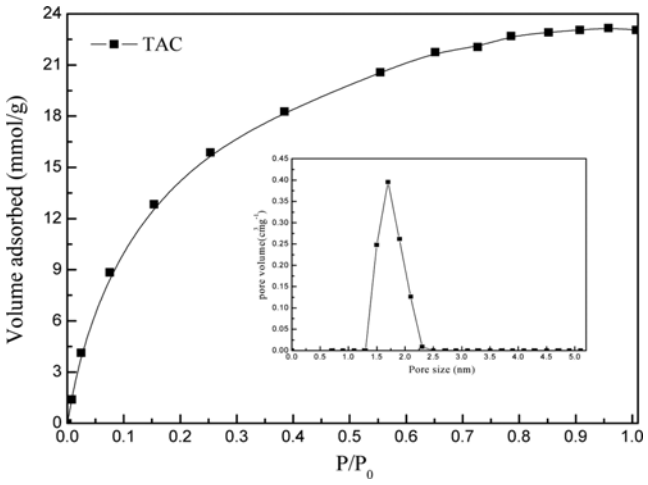

Fig. 1. N_2 adsorption isotherms and pore size distribution of TAC.

I adsorption isotherm according to the IUPAC classification [17]. The BET surface area and pore volume of TAC sample are 2,265 m^2/g and 1.60 cm^3/g, respectively. The pore size distributions calculated by density functional theory (DFT) prove that the pore size of TAC ranges from 1.25 to 2.25 nm. The huge surface area of the TAC provides the huge capacity for dye molecules' adsorption inside the pore structure.

3. Batch Equilibrium Studies

To study the effect of parameters such as contact time, initial concentration, solution pH, and temperature for the removal of dye molecules on TAC, batch experiments were conducted in a set of 250 mL stoppered flasks (Erlenmeyer flasks) that contain a definite volume (100 mL in each flask) of fixed initial concentrations (50-500 mg/L) of dyes solution. 0.02 g of each of the prepared TAC, with particle size of 150 μm, was added to each flask and kept in a shaker with 150 rpm at different temperatures (303, 313, 323, 333 K) for 4 h to reach equilibrium. The sample solutions were filtered at equilibrium using 0.45 μm filter paper to determine the residual concentrations. Then the samples were filtered and the residual concentrations of CV and NG in the filtrate were analyzed by a UV-Visible spectrophotometer (Shimadzu UV-160A) at maximum wavelengths (CV: λ_{max}=590 nm, NG: λ_{max}=714 nm). A series of dye solutions with various concentrations were used for the measurement of a calibration curve. A linear relationship between the absorbance and the dye concentration was obtained. The amount of dyes adsorbed at equilibrium condition, q_e (mg/g), was calculated as follows:

$$q_e = \frac{(C_o - C_e)\cdot V}{W} \quad (1)$$

where C_o and C_e (mg/L) are the initial and equilibrium concentrations of CV and NG solution, respectively; V (L) is the volume of solution, and W (g) is the weight of TAC used.

The linear form of Langmuir's isotherm model [18] is given by the following equation:

$$\frac{C_e}{q_e} = \frac{1}{q_L \cdot K_L} + \left(\frac{1}{q_L}\right)\cdot C_e \quad (2)$$

where q_L (mg/g) is the Langmuir maximum uptake of CV and NG per unit mass adsorbent, K_L (L/mg) is the Langmuir constant related to the rate of adsorption.

The well-known logarithmic form of the Freundlich model [19] is given by the following equation:

$$\ln q_e = \ln K_f + \left(\frac{1}{n}\right)\cdot \ln C_e \quad (3)$$

where K_f and n are Freundlich constants, with n indicating the favorableness of the adsorption process and K_f the adsorption capacity of the adsorbent. K_f can be defined as the adsorption or distribution coefficient and its represents the quantity of dye adsorbed onto activated carbon adsorbent for a unit equilibrium concentration. The slope 1/n ranging between 0 and 1, is a measure of adsorption intensity or surface heterogeneity, becoming more heterogeneous as its value gets closer to zero.

4. Adsorption Kinetics

In equilibrium experiments the q_e data are obtained at equilibrium, and in kinetic experiments the q_t data are obtained at different moments in time. The aqueous samples were taken at the desired time intervals, and the concentrations of CV and NG were similarly measured. The adsorbed amount of CV and NG at time t, q_t (mg/g), was calculated by:

$$q_t = \frac{(C_o - C_t)\cdot V}{W} \quad (4)$$

where C_t (mg/L) is the liquid-phase concentration of CV and NG solution at time t (min). Pseudo-first order model [20], pseudo-second order model [21], and intra-particle diffusion model [22] were used to analyze the kinetic data. These models can be derived as:

$$\text{Pseudo-first order model: } \ln(q_e - q_t) = \ln(q_e) - K_1 t \quad (5)$$

$$\text{Pseudo-second order model: } \frac{t}{q_t} = \frac{1}{K_2 q_e} + \frac{t}{q_e} \quad (6)$$

$$\text{Intra-particle diffusion model: } q_t = K_3 t^{1/2} \quad (7)$$

where q_e and q_t (mg/g) are the uptake of CV and NG at equilibrium and at time t (min), respectively, K_1 (1/min) is the adsorption rate constant, K_2 (g/mg.min) is the rate constant of second-order equation, K_3 (mg/g·min$^{1/2}$) is the intra-particle diffusion rate constant.

To quantitatively compare the applicability of different kinetic models in fitting to data, a normalized standard deviation, Δq (%), was calculated as below:

$$\Delta q(\%) = \frac{(q_{e,exp} - q_{e,cal})}{q_{e,exp}} \times 100\% \quad (8)$$

5. Adsorption Thermodynamics

Thermodynamic behavior of CV and NG adsorption onto TAC was evaluated by the thermodynamic parameters including the changes in free energy (G), enthalpy (H), and entropy (S). These parameters are calculated from the following equations:

$$\ln(K_d) = \frac{\Delta S}{R} - \frac{\Delta H}{RT} \quad (9)$$

$$\Delta G = -RT\ln(K_d) \quad (10)$$

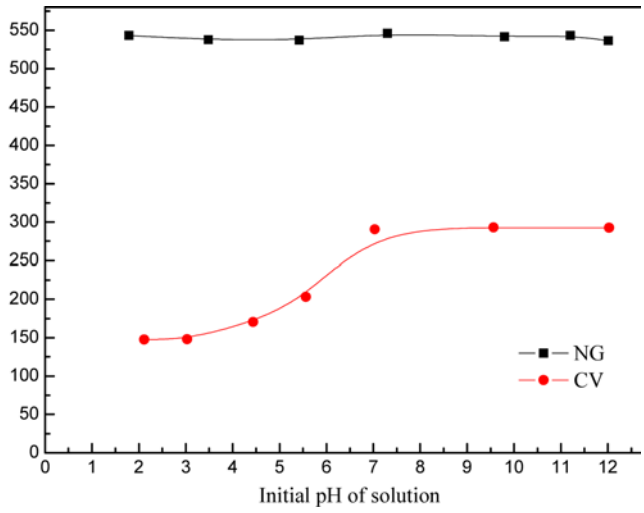

Fig. 2. Effect of pH on the adsorption of CV and NG onto TAC.

$$K_d = \frac{q_e(W/V)}{C_e} \quad (11)$$

where R is the universal gas constant 8.314 (J/mol K), T is the temperature (K), and K_d is the distribution coefficient for the adsorption.

RESULTS AND DISCUSSION

1. Effect of Solution Initial pH on Dye Uptake

Fig. 2 shows the effect of initial pH on the adsorption capacities of CV and NG on the TAC surface. It can be observed that the adsorption capacities of NG are slightly influenced by the pH in the range of 2-12. The adsorption capacities of CV quickly increased from 148 to 292 mg/g with increasing pH from 2 to 7 and remained unchangeable in the pH range of 7 to 12. Clearly, CV adsorption closely depends on the solution pH. The equilibrium adsorption q_e was found to increase with increasing pH. The mechanism of dye adsorption onto activated carbons is controlled by various factors, including physical and chemical properties and surface structure of activated carbons, molecular structure of dyes, hydrophobic interaction, electrostatic force, mass transfer process, etc. [22,23]. From Scheme 1, CV is a rigid molecule, while NG is more flexible in structure. The molecular structures of CV and NG are not changed in the pH range of 2-12. As can be seen from Fig. 2, the NG adsorption capacity (545 mg/g) onto TAC is larger than CV (292 mg/g) because NG should have more interaction sites with TAC because of its more flexible structure compared with CV. Electrostatic force could have more contribution to CV adsorption on TAC. Due to the stronger intermolecular forces between the flexible NG molecule and TAC surface, the adsorption capacity is slightly influenced by electrostatic force.

2. Adsorption Isotherms

Equilibrium data, commonly known as adsorption isotherms, describe how the adsorbate interacts with adsorbents, and give a comprehensive understanding of the nature of interaction. It is basically important to optimize the design of an adsorption system. The parameters obtained from the different models provide important information on the surface properties of the adsorbent and its

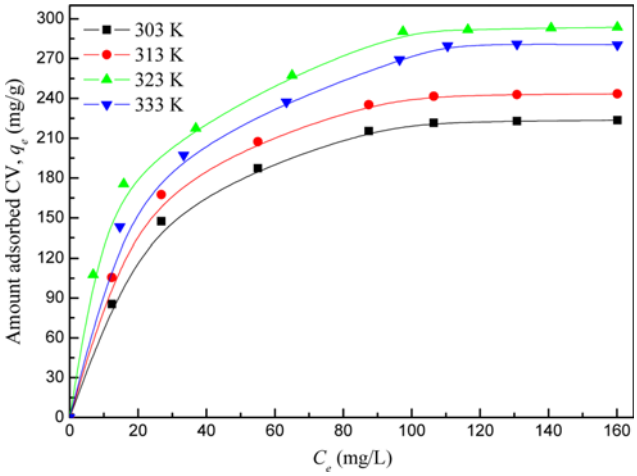

Fig. 3. Adsorption isotherms of CV on TAC at 303 K, 313 K, 323 K and 333 K, respectively.

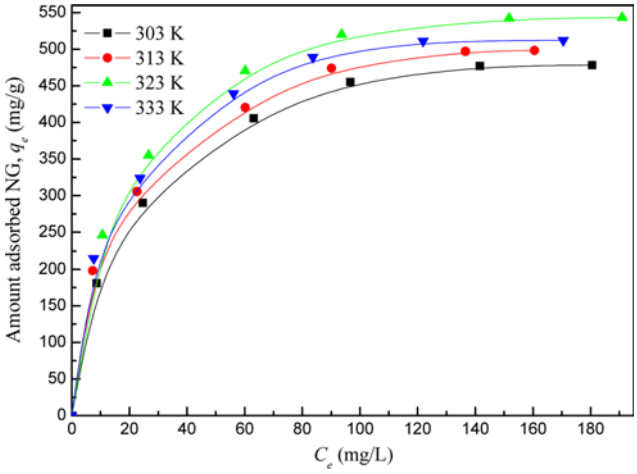

Fig. 4. Adsorption isotherms of NG on TAC at 303 K, 313 K, 323 K and 333 K, respectively.

affinity to the adsorbate. The Langmuir and Freundlich isotherms selected here are widely used to describe the dye adsorption at the solid-liquid interface.

The adsorption isotherms of CV and NG at different temperature (303 K, 313 K, 323 K and 333 K) and pH 7 on the TAC are presented in Figs. 3 and 4. The obtained experimental equilibrium adsorption data are then fitted using Langmuir and Freundlich isotherm models by Eq. (2) and Eq. (3). The calculated constants according to the two isotherm equations along with R^2 values (standard deviation) are presented in Table 1. This table shows that the Langmuir isotherm gives the best fitting with R^2>0.998. The good fitting to the Langmuir model for the dyes also suggests that the

Table 1. Constants and correlation coefficients of Langmuir and Freundlich models

Dye	Temperature (K)	Langmuir			Freundlich		
		q_L (mg/g)	K_L (L/mg)	R^2	K_f (L/g)	n	R^2
CV	303	259.067	0.0472	0.9984	39.0761	2.7249	0.9567
	313	245.098	0.0371	0.9965	26.5481	2.3293	0.9514
	323	291.545	0.0479	0.9987	38.2506	2.5169	0.9636
	333	285.714	0.0386	0.9983	41.5409	2.7428	0.9817
NG	303	531.915	0.0545	0.9995	95.9781	3.0488	0.9810
	313	492.611	0.0417	0.9994	61.7454	2.5207	0.9769
	323	543.478	0.0518	0.9995	96.3386	3.0325	0.9686
	333	512.821	0.0557	0.9991	84.8063	2.8361	0.9781

Table 2. Comparison of the maximum uptake capacities of CV and NG dyes on various adsorbents

Dye	Adsorbent	Maximum uptake capacities (mg/g)	Reference
CV	TAC	292	This work
	Sulfuric acid activated carbon	86	[26]
	Phosphoric acid activated carbon	60	[26]
	Activated carbon prepared from waste apricot	58	[27]
	Activated carbon from the waste biomass of wood apple rind	17	[28]
	Activated carbon derived from gölbaşı lignite	66	[29]
	Metal hydroxides sludge	40	[30]
	Clay minerals	800	[33]
NG	TAC	545	This work
	Metal hydroxides sludge	10	[30]
	Commercial activated carbon	130	[31]
	Layered double oxides	193	[32]

adsorption is limited with a monolayer coverage and the surface is relatively homogeneous. On the other hand, for TAC, the uptake capacity of NG is also significantly higher than that of the CV (approximately 1.9-fold higher). This may be due to the different molecule sizes and function groups of the two dyes. The larger dye molecule is difficult to penetrate into the adsorbent porous structure due to the pore blockage [24]. The adsorption capacities of CV and NG onto TAC in this work are summarized in Table 2, together with those of the adsorbents reported in the literature [25-32]. The TAC has relatively higher adsorption capacities of NG and CV compared with some other types of previously reported adsorbents [25-33]. Although CV has been reported to be efficiently removed by clay minerals [33], our TAC performance is comparable with the commercially available activated carbon [33] and superior to the activated carbon materials prepared by other researches [26-29]. These results reflect that the TAC is a potential adsorbent for adsorptive removal of CV and NG from aqueous solution.

3. Adsorption Kinetics

The effect of contact time on adsorption capacity of TAC to CV and NG at different temperature is shown in Figs. 5 and 6, respectively. These figures show that the adsorption capacity for CV and NG increases with the increase of contact time, and the adsorption reaches equilibrium within about 3 h. The saturation capacities of CV and NG are 242, 292, 283 mg/g; and 493, 545, 506 mg/g at 313 K, 323 K, and 333 K, respectively. These figures also show that rapid increase in adsorption capacity for the dyes is achieved during the first 1 h. The relative fast adsorption at the initial stage may be due to the availability of the uncovered surface area and the remaining active sites on the adsorbent.

The experimental kinetic data of CV and NG were correlated with three kinetic models: pseudo-first order, pseudo-second order and intra-particle diffusion models, according to Eqs. (5), (6) and (7). The calculated rate constants using the three kinetic equations along with R^2 values at different temperatures are presented in Table 3. As seen in Table 3, there is a large difference between the experimental and calculated adsorption capacity values when the pseudo-first model was applied. However, high R^2 values (more than 0.99) are obtained with the linear plot of t/q_t versus t, suggesting the pseudo-second order adsorption kinetics. Additionally, in comparison with the other two kinetic models, the pseudo-second order kinetic model predicts a better agreement between the experimental and calculated adsorption capacity values Δq (%). Identification of the rate-

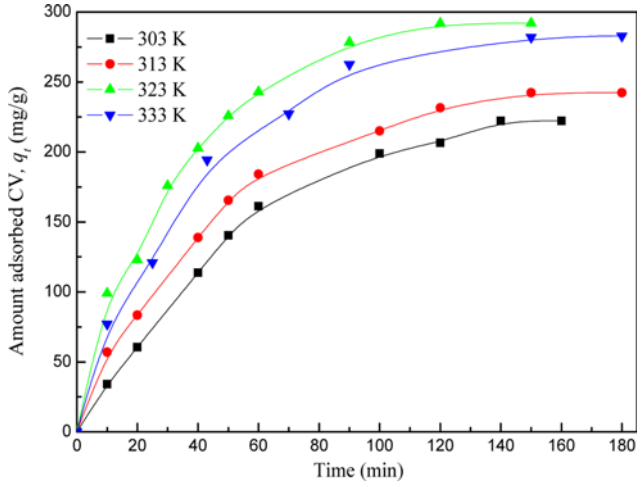

Fig. 5. Effect of contact time on the adsorption capacity of CV at 303 K, 313 K, 323 K and 333 K, respectively.

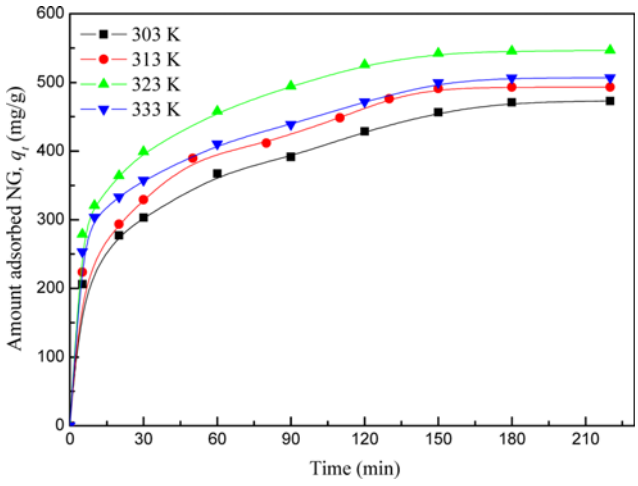

Fig. 6. Effect of contact time on the adsorption capacity of NG at 303 K, 313 K, 323 K and 333 K, respectively.

Table 3. Kinetic parameters for CV and NG adsorption on TAC

Temperature (K)	Pseudo-first-order rate equation							Pseudo-second-order rate equation						Intra-particle diffusion model			
	Dye	$q_{e,exp}$ (mg/g)	$q_{e,cal}$ (mg/g)	K_1 (1/min)	R^2	Δq (mg/g)	Δq (%)	$q_{e,exp}$ (mg/g)	$q_{e,cal}$ (mg/g)	K_2 (g/mg min)	R^2	Δq (mg/g)	Δq (%)	$q_{e,exp}$ (mg/g)	C (mg/g)	K_3 (mg/g $min^{1/2}$)	R^2
303	CV	223.53	254.81	0.023	0.9985	−0.14	0.06	223.53	171.89	2.3188	0.9941	51.64	23.10	223.53	19.243	20.655	0.9813
	NG	473.02	398.31	0.024	0.9439	74.71	15.79	473.02	356.98	28.11	0.9959	116.04	24.53	473.02	179.79	21.709	0.9861
313	CV	242.25	261.76	0.025	0.9909	−19.51	−8.05	242.25	334.45	0.0187	0.9946	−92.2	−38.06	242.25	14.683	18.937	0.9687
	NG	493.02	398.30	0.024	0.9439	94.72	19.21	493.02	500.00	0.0736	0.9958	−6.98	−1.42	493.02	199.798	21.709	0.9861
323	CV	291.83	317.16	0.033	0.9914	−25.33	−8.68	291.83	386.10	0.0281	0.9991	94.27	−32.30	291.83	46.037	22.658	0.9582
	NG	545.23	346.08	0.027	0.9709	199.15	36.53	545.23	549.45	0.1146	0.9979	4.22	−0.77	545.23	251.323	24.073	0.9835
333	CV	282.83	302.53	0.028	0.9821	−19.7	−6.97	282.83	348.43	0.0268	0.9961	−65.6	−23.19	282.83	34.841	20.663	0.9519
	NG	506.40	297.73	0.021	0.9589	208.67	41.21	506.40	490.20	0.1220	0.9976	16.2	3.20	506.40	228.917	21.907	0.9909

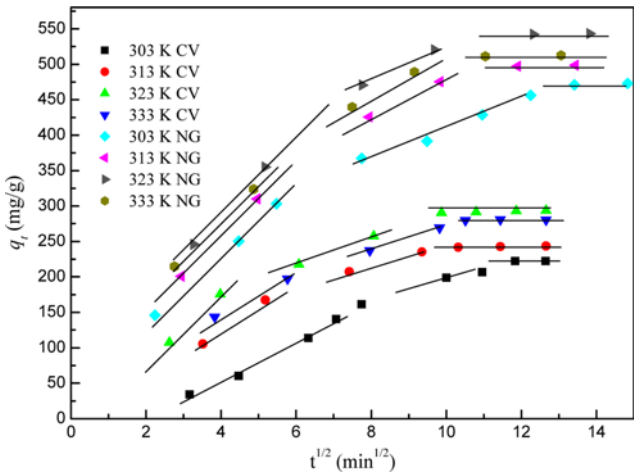

Fig. 7. Weber-Morris intra-particle diffusion plots for the adsorption of CV and NG on TAC.

limiting step is important in proper design of the adsorbents. The Weber-Morris model, which is widely used to describe the rate control process, suggests that the adsorption is controlled by intraparticle diffusion with more than two stages. When the plots do not pass through the origin, this is indicative of some degree of boundary layer control, suggesting that intraparticle diffusion is not the only rate controlling step, but also other processes may control the rate of adsorption [32]. The slowest stage controls the overall rate of the adsorption process. Fig. 7 presents the plots of q_t versus $t^{0.5}$ for CV and NG adsorption on TAC and distribution of data could be represented by three lines. Multilines indicate that the adsorption rate of CV and NG was controlled by three adsorption stages. The first line at the beginning of adsorption represents the external mass transfer with a high adsorption rate. The second line indicates the role of intraparticle diffusion on the adsorption rate. The last line indicates the final equilibrium stage where intraparticle diffusion starts to slow due to the saturation of the TAC adsorption site by adsorbates and possibly lowered adsorbate concentration left in the aqueous solution. Such finding is similar to that made in previous works on adsorption [34-36].

4. Effect of Solution Temperature and Adsorption Thermodynamics

Temperature has a very significant influence on the adsorption process because a change in temperature will cause large changes in the adsorption equilibrium capacity of the adsorbent for a particular adsorbate. Adsorption experiments were carried out at four different temperatures (303 K, 313 K, 323 K, 333 K) to investigate the effect of adsorption temperature on the adsorption capacity of CV and NG on TAC. As can be seen from Figs. 3-6, the dye (CV and NG) adsorption capacities increased as the temperature increased from 303 K to 323 K. As is known from Table 4, the ΔH parameters are positive for CV and NG adsorption on TAC, which indicates that higher temperature is favorable for adsorption. The negative ΔG values indicate thermodynamically spontaneous nature of the adsorption. The decrease in ΔG values at further increased temperature of 333 K shows a decrease in feasibility of adsorption. The positive ΔS value suggests a compensation for the adsorption enthalpy to favor the adsorption thermodynamics.

Table 4. Thermodynamics adsorption parameters for CV and NG on TAC

Dye	ΔH (kJ/mole)	ΔS (J/mole)	ΔG (kJ/mole)			
			303 K	313 K	323 K	333 K
CV	17.44	112.91	−16.66	−17.96	−19.27	−18.95
NG	6.20	81.16	−18.39	−19.18	−20.05	−20.80

On the basis of adsorption isotherms, the data calculated with Eq. (1) were used to calculate the value of K_d from Eq. (11) at each temperature [37]. Then, the ΔG parameters were calculated from Eqs. (10), and according to Eqs. (9) the ΔH and ΔS parameters for CV and NG adsorption were derived from the slope and intercepts of the plot of $\ln(K_d)$ versus 1/T. The calculated values of ΔH, ΔS, and ΔG are listed in Table 4. The obtained values for Gibbs free energy change (ΔG) are −16.66 and −18.39, −17.96 and −19.18, −19.27 and −20.05, −18.95 and −20.80 kJ/mole for CV and NG adsorption on TAC at 303, 313, 323 and 333 K, respectively. The negative ΔG values indicate the thermodynamically spontaneous nature of the adsorption. The decrease in ΔG values with increasing temperature shows a decrease in feasibility of adsorption at higher temperatures. The ΔH parameters are 17.44 and 6.20 kJ/mole for CV and NG adsorption on TAC, respectively. The positive ΔH is an indicator of the endothermic nature of the adsorption and its magnitude also gives information on the type of adsorption, which can be either physical or chemical. Usually, an adsorption enthalpy ranging from 2.1 to 20.9 kJ/mol corresponds to physical adsorption [38]. Physical adsorption occurs when the intermolecular attractive forces between the molecules of adsorbate and adsorbent are greater than those between the adsorbate themselves. Physical adsorption, which may be a monomolecular or multi-molecular layer, occurs rapidly. In contrast, chemisorption involves the formation of chemical bonds between the adsorbate and adsorbent. It takes place only at high temperatures and may be slow [38]. In this study, the adsorption heat of CV and NG is in the range of physical adsorption. The ΔS values are 112.91 and 81.16 J/mole for CV and NG adsorption on TAC, respectively. The positive ΔS value suggests an increase in the randomness at adsorbent-solution interface during the adsorption process.

CONCLUSIONS

The present work reveals that the skin residues of torreya grandis, which is an abundantly available industrial waste, can be easily converted into good adsorbent (TAC) for removal of dyes from industrial wastewater. The maximum equilibrium adsorption capacities were 292 mg/g and 545 mg/g for CV and NG, respectively, which is higher than some of the other types of adsorbents reported in the literature. The adsorption of and naphthol green dye using activated carbon (TAC) is more efficient than crystal violet dye from aqueous solution. On applying pseudo-first-order, pseudo-second-order kinetics and intra-particle diffusion models to the adsorption of the dyes on TAC, it was found that the interactions could be better explained by pseudo-second-order kinetics. Using TAC

material as an adsorbent, the advantage is twofold: It not only acts as an effective and economic adsorbent as compared to some other existing adsorbents for solving the problem of color pollution, but also opens a new way of re-utility of industrial sludge waste disposal.

ACKNOWLEDGEMENT

This work was supported by the Public Projects of Zhejiang Province of China (No. 2013C31094), Zhejiang Qianjiang Talent Project (No. QJD1302014) and the Open Research Fund of Top Key Discipline of Chemistry in Zhejiang Provincial Colleges and Key Laboratory of the Ministry of Education for Advanced Catalysis Materials (Zhejiang Normal University, P.R. China).

REFERENCES

1. G. Crini, *Bioresour. Technol.*, **97**, 1061 (2006).
2. B. H. Hameed and A. A. Rahman, *J. Hazard. Mater.*, **160**, 576 (2008).
3. P. Vandevivere, R. Bianchi and W. Verstraete, *J. Chem. Technol. Biotechnol.*, **72**, 289 (1998).
4. Y. Slokar and A. L. Marechal, *Dyes Pigm.*, **37**, 335 (1998).
5. S. Wang, Z. H. Zhu, A. Coomes, F. Haghseresht and G. Q. Lu, *J. Colloid Interface Sci.*, **284**, 440 (2005).
6. D. Prahas, Y. Kartika, N. Indraswati and S. Ismadji, *Chem. Eng. J.*, **140**, 32 (2008).
7. M. P. Elizalde-González, J. Mattusch and R. Wennrich, *Bioresour. Technol.*, **99**, 5134 (2008).
8. R. Zhu, Q. Chen, H. Liu, F. Ge, L. Zhu, J. Zhua and H. He, *Appl. Clay Sci.*, **88-89**, 33 (2014).
9. I. D. Mall, V. C. Srivastava and N. K. Agarwal, *Dyes Pigm.*, **69**, 210 (2006).
10. A. E. Ofomaja, *Chem. Eng. J.*, **143**, 85 (2008).
11. B. H. Hameed, *J. Hazard. Mater.*, **154**, 204 (2008).
12. Y. Cao, H. Zhu and X. Wang, *J. Zhejiang Normal Univ. China*, **31**, 190 (2008).
13. L. Wang, X. Chen, Y. Dong and H. Lu, *Acta Agriculturae Zhejiangensis*, **22**, 229 (2010).
14. X. Sun, W. Dai, H. Lv, Y. Du, R. Gong and J. Hu. *China Patent,* CN103288083A (2013).
15. L. Ai, C. Zhang and L. Meng, *J. Chem. Eng. Data*, **56**, 4217 (2011).
16. B. H. Hameed, A. T. M. Din and A. L. Ahmad, *J. Hazard. Mater.*, **141**, 819 (2007).
17. J. Yi and L. Zhang, *Bioresour. Technol.*, **99**, 2182 (2008).
18. I. Langmuir, *J. Am. Chem. Soc.*, **38**, 2221 (1916).
19. H. M. F. Freundlich, *Z. Phys. Chem.*, **57**, 385 (1906).
20. S. Langergen and B. K. Svenska, *Veteruskapsakad Handlingar*, **24**, 1 (1898).
21. Y. S. Ho and G. Mckay, *Process Biochem.*, **34**, 451 (1999).
22. G. Annadurai, R. S. Juang and D. J. Lee, *J. Hazard. Mater.*, **92**, 263 (2002).
23. S. Chen, J. Zhang, C. Zhang, Q. Yue, Y. Li and C. Li, *Desalination*, **252**, 149 (2010).
24. L. C. Juang, C. C. Wang and C. K. Lee, *Chemosphere*, **64**, 1920 (2006).
25. S. Senthilkumaar, P. Kalaamani and C. V. Subburaam, *J. Hazard. Mater.*, **136**, 800 (2006).
26. C. Akmil-basar, *J. Hazard. Mater.*, **135**, 232 (2006).
27. R. Malarvizhi and Y. S. Ho, *Desalination*, **264**, 97 (2011).
28. D. Tolga, R. K. Ali, O. Yunus, D. Erkan, A. Salih and Z. F. Turkmenoglu, *Physicochem. Probl. Miner. Process.*, **48**, 253 (2012).
29. M. F. Attallah, I. M. Ahmed and M. M. Hamed, *Environ. Sci. Pollut. Res. Int.*, **20**, 1106 (2013).
30. B. M. Elzbieta and D. Adamczyk, *Rocznik ochrona srodowiska*, **15**, 966 (2013).
31. F. Zhang, Z. Ni, S. Xia, X. Liu and Q. Wang, *Chinese J. Chem.*, **27**, 1767 (2009).
32. K. G. Bhattacharyya and A. Sharma, *Dyes Pigm.*, **65**, 51 (2005).
33. J. Wei, R. Zhu, J. Zhu, F. Ge, P. Yuan, H. He and C. Ming, *J. Hazard. Mater.*, **166**, 195 (2009).
34. K. G. Bhattacharyya and A. Sharma, *J. Hazard. Mater.*, **113**, 97 (2004).
35. K. Mahmoudi, N. Hamdi, A. Kriaa and E. Srasra, *Russian J. Phys. Chem. A.*, **86**, 1294 (2012).
36. N. E. Q. Emad, S. J. Allen and G. M. Walker, *Chem. Eng. J.*, **124**, 103 (2006).
37. S. Karagoz, T. Tay, S. Ucar and M. Erdem, *Bioresour. Technol.*, **99**, 6214 (2008).
38. Z. Belala, M. Jeguirim, M. Belhachemi, F. Addoun and G. Trouvé, *Desalination*, **271**, 80 (2011).